




Cite this: *Phys. Chem. Chem. Phys.*, 2020, 22, 2841

# A well-isolated vibrational state of CO<sub>2</sub> verified by near-infrared saturated spectroscopy with kHz accuracy†

Hao Wu,<sup>a</sup> Chang-Le Hu,<sup>a</sup> Jin Wang,<sup>a</sup> Yu R. Sun,<sup>ab</sup> Yan Tan,<sup>ab</sup> An-Wen Liu <sup>\*ab</sup> and Shui-Ming Hu<sup>ab</sup>

Quantitative determination of atmospheric CO<sub>2</sub> concentration by remote sensing relies on accurate line parameters. Lamb dips of the lines up to  $J'' = 72$  in the 30013–00001 band at 1605 nm were measured using a comb-locked cavity ring-down spectrometer, and the positions were determined with an accuracy of a few kHz. A simple effective Hamiltonian model can fit the rotational energies in the 30013 state ideally within the experimental accuracy, indicating that the vibrational state is well-isolated and can be regarded as free from perturbations. From a comparison between other bands using a similar analysis, we conclude that the transitions in the 30013–00001 band could be more suitable as reference lines for sensing applications with the potentially improved line parameter accuracy.

Received 17th September 2019,  
 Accepted 3rd January 2020

DOI: 10.1039/c9cp05121j

[rsc.li/pccp](http://rsc.li/pccp)

## 1. Introduction

Carbon dioxide and methane play critical roles in global warming, as long-lived and major greenhouse gases in the Earth's atmosphere. Several passive remote sensors or IPDA LIDAR are used or are to be launched to monitor the atmospheric column densities of CO<sub>2</sub> (OCO-2<sup>1</sup> and GOSAT<sup>2</sup>) and CH<sub>4</sub> (GOSAT and MERLIN<sup>3</sup>), for the detection of the long-term change, and the estimation of sources and sinks of global carbon. Quantitative analysis requires sufficiently accurate reference data of the line parameters of several atmospheric molecules.<sup>4</sup> For example, high-resolution spectroscopy of CO<sub>2</sub> at 1.6 μm and 2.06 μm, and the O<sub>2</sub> A-band at 0.76 μm were recorded to retrieve highly accurate line parameters for the OCO-2 project. The absolute transition frequency can be easily measured with an accuracy better than a few MHz<sup>5–8</sup> with the help of an optical frequency comb (OFC),<sup>9</sup> while the difficulty in retrieving line intensity and line profile parameters increases quickly with precision.<sup>10–14</sup> Furthermore, discrepancies between different experimental results reach 1%,<sup>11</sup> which motivated theoretical studies based on first-principles,<sup>10,15,16</sup> or effective Hamiltonian and effective dipole moment surface models.<sup>17</sup> Agreements between the UCL *ab initio* calculations and highly accurate experiments are at the 0.5% level for the

transitions in the 30013–00001<sup>10</sup> and 20012–00001<sup>12,13</sup> bands. The discrepancy increases to 1.7–3.6% for the transitions in the 30012–00001 band<sup>18</sup> in comparison with the line intensities measured with Fourier-transform spectroscopy. The recent highly accurate measurements with a frequency-stabilized cavity ring-down spectrometer also show that the deviations from the UCL values are –1.14% and –3.80% for the R(16)<sup>14</sup> and P(32)<sup>19</sup> lines in the 30012–00001 band, respectively. The disagreements are larger than the calculated accuracy of 0.5% claimed by the UCL group for this most atmospherically interesting CO<sub>2</sub> (“stable”) band. This inconsistency inspired us to reconsider the accuracy limit of the Lodi–Tennyson methodology.<sup>20</sup> For which band can the line parameters be potentially calculated with superior accuracy?

Herein, we present a method to find weak resonances in a vibrational band by the analysis of line positions at an accuracy of a few kHz. Local deviations in the positions with successive  $J$  numbers can be used as a sensitive indicator of the presence of perturbations, such as the local perturbations revealed in the excited vibrational state levels of acetylene.<sup>21,22</sup> For CO<sub>2</sub>, accuracies at dozens of kHz have been achieved by saturated spectroscopy measurements in the mid-infrared region,<sup>7,23–33</sup> and hundreds of kHz uncertainties by Doppler-limited absorption spectroscopy in the near-infrared region.<sup>5,6,12,34</sup> Only the line positions in the 00011–00001,<sup>27,29</sup> 10011–00001,<sup>28</sup> 10012–00001,<sup>25</sup> 30012–00001,<sup>5</sup> and 30013–00001<sup>6,7</sup> bands have been measured for serial transitions from P- and R-branches. Here we report Doppler-free saturation spectroscopy of <sup>12</sup>C<sup>16</sup>O<sub>2</sub> ro-vibrational transitions in the 30013–00001 cold band near 1.605 μm for P(72)–R(70) 72 lines recorded using a comb-locked cavity ring-down spectrometer.<sup>35</sup>

<sup>a</sup> Hefei National Laboratory for Physical Sciences at Microscale, iChem Center, University of Science and Technology of China, Hefei, 230026, China.  
 E-mail: awliu@ustc.edu.cn

<sup>b</sup> CAS Center for Excellence in Quantum Information and Quantum Physics, University of Science and Technology of China, Hefei 230026, China

† Electronic supplementary information (ESI) available. See DOI: 10.1039/c9cp05121j

The absolute transition frequencies were determined to a few kHz for these lines with a wide intensity range by three orders of magnitude. The detection limit (noise-equivalent absorption coefficient) reached  $4.6 \times 10^{-13} \text{ cm}^{-1}$ , which allowed us to detect Doppler-free saturation spectra of extremely weak transitions.<sup>36</sup> To the best of our knowledge, it is the first time that transitions weaker than  $1 \times 10^{-26} \text{ cm molecule}^{-1}$  have been determined with an accuracy of a few kHz. The fit of the ground combination differences resulted in a new set of ground state constants, which was used to improve the molecular spectroscopic parameters of the 00011, 10011, 10012, 30012, and 30013 vibrational states. Differences between the calculated and observed line positions allow us to trace weak resonances in these bands, and to propose the line parameters of which band can be potentially improved for remote sensing applications.

## 2. Experimental setup

The experimental setup is shown in Fig. 1, which is similar to our recently developed comb-locked cavity ring-down saturation spectrometer described in detail in ref. 35–37. A tunable external-cavity diode laser (ECDL, Toptica DL Pro-1550) is used as the probe laser, being locked to a ring-down (RD) cavity using the Pound–Drever–Hall (PDH) method. The RD cavity is made of Invar and composed of a pair of high-reflectivity (HR) mirrors ( $R = 99.997\%$  at  $1.54\text{--}1.7 \mu\text{m}$ , Layertec GmbH Inc.) with a distance of  $108.0 \text{ cm}$ , leading to a free spectral range (FSR) of  $138.86 \text{ MHz}$ , a finesse of  $1.36 \times 10^5$ , and a mode width of about  $1.0 \text{ kHz}$ . The RD cavity is temperature stabilized at  $297.85 \text{ K}$ , with a fluctuation below  $10 \text{ mK}$ . The cavity length is stabilized through a piezo actuator (PZT) driven by a phase-lock circuit based on the beat signal between the probe laser and an optical frequency comb. The frequency comb is synthesized by an Er-fiber oscillator operated at  $1.56 \mu\text{m}$ . The repetition frequency ( $f_{\text{rep}} \approx 184 \text{ MHz}$ ) and carrier offset frequency ( $f_0$ ) of the comb are locked to precise radio-frequency sources, both referenced to a Global Positioning System (GPS)-disciplined rubidium clock (SRS FS725). A separated p-polarization probe laser beam,

frequency shifted by two acousto-optic modulators (AOM), is coupled into the RD cavity from another side of the cavity and used to produce the ring-down signal. The frequency locking and spectral probing laser beams are separated with a combination of polarizing waveplates and Glan–Taylor prisms. The laser power used for spectral probing was about  $1.5 \text{ mW}$  resulting in the intra-cavity laser powers of  $7\text{--}17 \text{ W}$ <sup>35,38</sup> for 72 measured transitions at respective pressures.

One of the AOMs serves as a beam chopper, which is triggered by an external rectangle wave to shut off the CRDS-probing beam to initial a ring-down event. The ring-down curve is fit by an exponential decay function to derive the decay time  $\tau$ , and the sample absorption coefficient  $\alpha$  is determined from the change of the cavity loss rate:  $\alpha = (c\tau)^{-1} - (c\tau_0)^{-1}$ , where  $c$  is the speed of light, and  $\tau$  and  $\tau_0$  are decay times of the cavity with and without sample, respectively. The minimum detectable absorption coefficient reaches about  $6.5 \times 10^{-12} \text{ cm}^{-1}$  at an averaging time of  $1 \text{ s}$ . The saturated absorption spectra are measured by tuning the reference frequency  $f_B$  of the phase-lock loop:

$$\nu = f_0 + N \times f_{\text{rep}} + f_B + 2f_{\text{AOM}} \quad (1)$$

where  $f_{\text{AOM}}$  is the radio frequency driving two AOMs.

## 3. Results and discussions

### A. Absolute frequencies of 72 lines in the 30013–00001 band

A carbon dioxide gas sample in natural abundance was used with a “freeze–pump–thaw” purification before measurement. As given in the HITRAN2016<sup>39</sup> database, the line intensities vary in the range of  $6.4 \times 10^{-27}\text{--}1.8 \times 10^{-23} \text{ cm molecule}^{-1}$  for the 72 lines, P(72)–R(70) in the 30013–00001 band of  $^{12}\text{C}^{16}\text{O}_2$ . Doppler-free Lamb-dip spectra were recorded at four pressures ( $0.3, 1.0, 1.6, \text{ and } 2.2 \text{ Pa}$ ) depending on the intensities of the transitions. A single exponential decay function was applied to fit the RD signal on the purpose of the precise line position determination in spite of the non-exponential shape in the saturated regime.<sup>30</sup> The noise level is about  $2.6 \times 10^{-11} \text{ cm}^{-1}$  for one spectral scan accomplished in about  $60 \text{ s}$ . Fig. 2 shows the averaged spectra of the P(16) and P(72) lines over a span of  $4.0 \text{ MHz}$ . The spectra were fit with a Lorentzian function for the saturated absorption with the corresponding residuals illustrated in the lower panels of Fig. 2. The RMS value of the residuals reaches  $4.6 \times 10^{-13} \text{ cm}^{-1}$  for the P(72) spectrum averaged from 2000 scans recorded in over 24 hours, which is comparable to the best-reported detection limit of CRDS.<sup>40</sup> The simulated spectrum of the P(72) line yielded a width (full width at half maximum, FWHM) of about  $660 \text{ kHz}$  and a dip depth of  $1.6 \times 10^{-11} \text{ cm}^{-1}$ , leading to a signal-to-noise ratio of about 30. The amplitude of the fitting residual around the peak center of P(16) is about 3% of the depth of the Lamb dip, which cannot be accounted for in a symmetric Lorentzian profile.

Fig. 3 shows the measured Lamb-dip depths for 72 lines ( $-72 \leq m \leq 71$ ) in the 30013–00001 band at respective experimental pressures, where the quantum number  $m$  of the lower state is  $-J$  in the P-branch and  $J + 1$  in the R-branch.

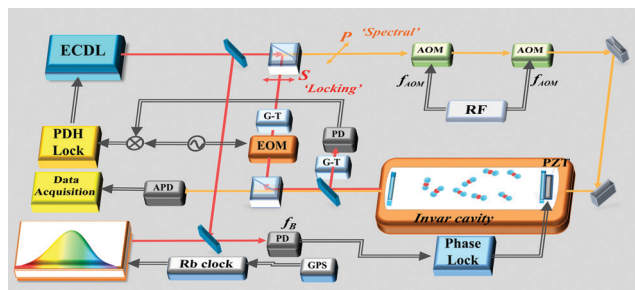


Fig. 1 Schematic of the experimental setup. The s-polarized beam from an ECDL laser is PDH-locked with the cavity. The p-polarized beam from the probe laser (referred to as “spectral” beam) is frequency shifted and used for CRDS measurement. The ring-down cavity length is locked through the beating signal between the probe and a frequency comb. Abbreviations: AOM: acousto-optic modulator; EOM: electro-optic modulator; G–T: Glan–Taylor prism; PZT: piezo actuator; Ol: optical isolator.

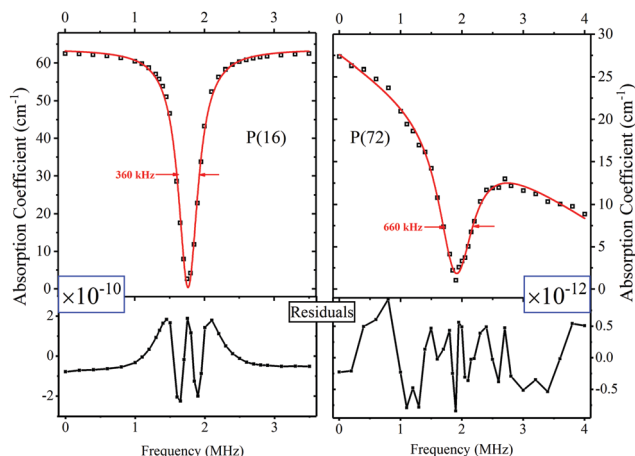


Fig. 2 Cavity ring-down saturation spectra of the P(16) (left panel) and P(72) (right panel) lines in the 30013–00001 band of  $^{12}\text{C}^{16}\text{O}_2$  recorded at sample pressures of 0.3 Pa and 1.6 Pa, respectively. The lower panels show the residuals of the fit using a Lorentzian profile.

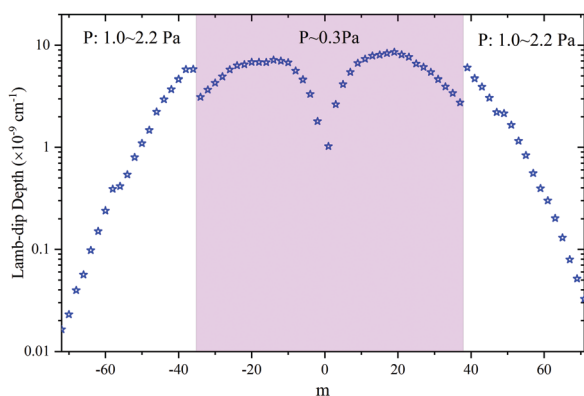


Fig. 3 Measured Lamb-dip depths of the P(72)–R(70) 72 lines in the 30013–00001 band of  $^{12}\text{C}^{16}\text{O}_2$  recorded at sample pressures in the range of 0.3–2.2 Pa.

The dip depths of 72 lines distribute in the range of  $1.6 \times 10^{-11}$ – $8.6 \times 10^{-9} \text{ cm}^{-1}$  by two magnitudes with estimated saturation parameters  $S$  of about 0.12–0.60 according to the equations given in ref. 35.

A summary of the estimated systematic uncertainties is presented in Table 1 for 72 observed lines associated with the

statistical errors of the line centers. The uncertainty budgets were given as Set I, II, and III for 34 strong ( $> 5 \times 10^{-24} \text{ cm molecule}^{-1}$ ), 18 middle, and 20 weak ( $< 5 \times 10^{-25} \text{ cm molecule}^{-1}$ ) lines, respectively. The statistical uncertainties are less than 12 kHz for all the studied lines.

The systematic uncertainties mainly came from the seven sources listed in Table 1, followed by detailed discussions. The frequency comb used for calibration has an uncertainty of 0.4 kHz around 1.6  $\mu\text{m}$  due to the long-term stability of  $2 \times 10^{-12}$  from the GPS-disciplined rubidium clock. Similar to that discussed in our previous studies,<sup>35–37,41,42</sup> the uncertainty in the range of 0.2–25 kHz was assigned for the possible asymmetry in the model of the line profile. The frequency shift due to the bias in the cavity locking servo is about 0.4 kHz estimated from the Allan deviation of the beat frequency between the probe laser and the frequency comb. The uncertainty in the driving frequencies of the AOMs is negligible. Taking a root-square-mean velocity of 411  $\text{m s}^{-1}$  of the  $^{12}\text{C}^{16}\text{O}_2$  molecule at 298 K, the second-order Doppler shift is 0.18 kHz with an uncertainty below 10 Hz. Under a laser power of 18 W inside the cavity, the AC Stark shift is negligible for all 72  $\text{CO}_2$  lines. Note that contrary considerations of the pressure shifts were used in the study by Burkart *et al.*<sup>7</sup> and in this work. The corrections of pressure shifts based on the self- and air-shifts obtained from a Doppler-limited spectrum<sup>43</sup> were included for 10 line positions of P(16)–P(42) of  $\text{CO}_2$  in the 30013–00001 band. However, we did not find evidence of a pressure shift under a pressure of less than 3 Pa in the studies of  $\text{CO}$ ,<sup>37</sup>  $\text{C}_2\text{H}_2$ ,<sup>41</sup> and  $\text{HD}$ .<sup>36</sup> A series of measurements were carried out to investigate the pressure shifts under different experimental pressures for three lines with two orders of intensity dynamic. As shown in Fig. 4, the pressure shifts of the P(2), P(16) and R(54) lines were determined to be  $-0.52 \pm 0.45$ ,  $-0.18 \pm 0.23$ , and  $-0.38 \pm 0.80 \text{ kHz Pa}^{-1}$  through a linear fit of results derived from 200 scans at different pressures. The pressure shifts were reported to be  $-0.94$ ,  $-1.71$ , and  $-2.8 \text{ kHz Pa}^{-1}$  in the Doppler regime for these lines,<sup>11</sup> indicating significant differences. In the meantime, the self-pressure broadening width at the low pressure is around 120–160  $\text{kHz Pa}^{-1}$ , which is 60–280% larger than those in the Doppler contour for these three transitions.<sup>39</sup> The non-linear dependence of the self-broadening width and pressure-induced shift on the gas pressure were first observed in the saturated absorption of  $\text{CH}_4$  around 3.39  $\mu\text{m}$ .<sup>44</sup> The collisional

Table 1 Uncertainty budget, 72 lines in the 30013 ← 00001 band of  $^{12}\text{C}^{16}\text{O}_2$ . (unit: kHz)

		Frequency shift	Uncertainty		
			I strong	II middle	III weak
Statistics			0.2–0.4	0.2–2.3	1.4–12
Systematic Source		Frequency comb	0.4	0.4	0.4
		Line profile asymmetry	0.2–0.8	1.6–2.2	1.4–25
		Cavity locking servo	0.4	0.4	0.4
		AOM frequency	0.05	0.05	0.05
		Pressure shift	0.23	0.45	0.80
		Power shift	0.0	0.37	0.37
		Second order Doppler	0.18	<0.01	<0.01
Total		0.18	0.7–1.1	1.0–2.3	2.1–28

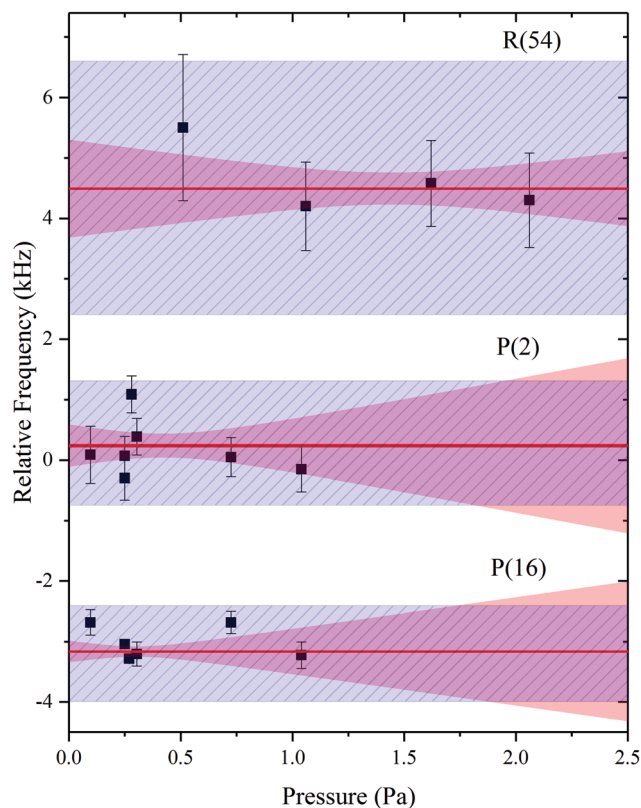


Fig. 4 Relative line centers of P(2), P(16) and R(54) derived from spectra recorded under different sample pressures. The blue shades show the uncertainties of line positions for each line, and the red areas show 68% confidence intervals for the linear fit with pressure shifts.

broadening coefficient of  $\text{CH}_4$  decreases from  $225 \text{ kHz Pa}^{-1}$  in the pressure range of 0.1 Pa to  $49 \text{ kHz Pa}^{-1}$  in the Doppler regime, while the collisional shift at lower pressures decreased by about an order of magnitude compared to those in the region high pressures.<sup>45</sup> The similar nonlinear dependence of collisional broadening in gases was observed in  $\text{NH}_3$ ,<sup>46</sup>  $\text{CO}_2$ ,<sup>47,48</sup>  $\text{SF}_6$ <sup>49</sup> and  $\text{C}_2\text{H}_2$ .<sup>50</sup> A detailed theoretical analysis of resonance shifts under lower pressures can be found in ref. 51 and 52 by Alekseev *et al.* For simplicity, we use the average of the positions at sample pressures in the range of 0.3–2.2 Pa.

Three sets of uncertainties of 0.23 kHz (I), 0.45 kHz (II), and 0.8 kHz (III) are left for the lines in the different intensity regions in case of possible contribution from the pressure shift. No power dependence was observed within the experimental uncertainty by the measurements of the P(2) line position at different input powers at a fixed pressure of 0.3 Pa, similar to our previous Lamb-dip studies of  $\text{CO}$ ,<sup>37</sup>  $\text{C}_2\text{H}_2$ ,<sup>41</sup> and  $\text{H}_2\text{O}$ .<sup>42</sup>

The positions of 72 lines in the 30013–00001 band of  $\text{CO}_2$ , together with the uncertainties, are given in the (ESI†). Fig. 5 shows the comparison of transition frequencies obtained in this work and those recently reported by Long *et al.*<sup>6</sup> with Doppler-limited (red square) and by Burkart *et al.*<sup>7</sup> with Doppler-free Lamb-dip (blue triangle) measurements. The error bars represent the  $1\text{-}\sigma$  standard uncertainties by combining the experimental uncertainty from this work and respective

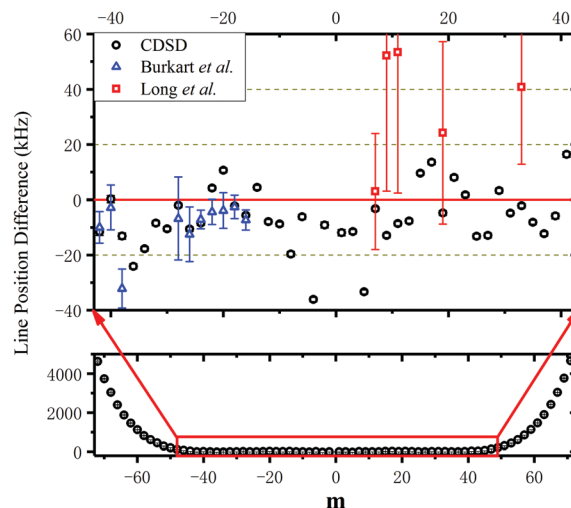


Fig. 5 Line position difference between this work and those from Long *et al.*,<sup>6</sup> Burkart *et al.*,<sup>7</sup> and the carbon dioxide spectroscopic databank CDS2019.<sup>17</sup>

literature values. A good agreement can be found between ours and Burkart's Lamb-dip studies except for the P(38) transition with a deviation over four times the combined uncertainty. Our results confirm the stated uncertainties of several tens of kHz for most lines from Long's measurement. While two data points for the R(16) and R(26) lines are missed in the plot due to more significant deviations ( $-219 \pm 32$ ) kHz ( $6.8\sigma$ ) and ( $-124 \pm 18$ ) kHz ( $6.9\sigma$ ), respectively. We also compared the line frequencies archived in the latest carbon dioxide spectroscopic databank (CDS2019).<sup>17</sup> Note that the CDS2019 line positions rely on the experimental values, and were improved with the Lamb-dip measurements by Burkart *et al.*<sup>7</sup> in the 30013–00001 band. The empirical  $\text{CO}_2$  transition frequencies agree very well with our measurements with differences around 20 kHz for ( $-44 \leq m \leq 43$ ), and the difference increases with  $J''$  (rotational quantum number of lower state) and reaches 4.6 MHz for  $J'' = 72$ .

## B. Spectroscopic analysis of Ro-vibrational transition frequencies

A simple model of unperturbed rotational energies in a well-isolated vibrational band was used to analyze the line positions:

$$E(J) = G_v + B_v J(J+1) - D_v J^2(J+1)^2 + H_v J^3(J+1)^3 + L_v J^4(J+1)^4 + M_v J^5(J+1)^5 + N_v J^6(J+1)^6 + O_v J^7(J+1)^7 + \dots \quad (2)$$

where  $G_v$  is the vibrational term and  $B_v$ ,  $D_v$ ,  $H_v$ ,  $L_v$ ,  $M_v$ ,  $N_v$ , and  $O_v$  are rotational and centrifugal distortion constants. As a symmetric molecule without microwave absorption, the ground state energies of the  $^{12}\text{C}^{16}\text{O}_2$  molecule were derived by fitting precise line positions in several infrared cold bands.<sup>6,8,25,27,29</sup> However, most ground state energies cannot be reproduced very well by the most recent two sets of spectroscopic constants.<sup>6,25</sup> The difference reaches about 78 kHz with  $J = 72$ , which is far beyond our experimental uncertainty.

As the ground state parameters retrieved with the saturated absorption spectroscopy in the near-infrared regions for  $^{12}\text{C}_2\text{H}_2$ <sup>53</sup>

and  $^{13}\text{C}_2\text{H}_2$ <sup>54,55</sup> molecules with  $D_{\infty h}$  symmetry, the ground state spectroscopic constants of  $^{12}\text{C}^{16}\text{O}_2$  can also be improved by fitting 67 ground combination differences determined from saturation measurements (this work and those in ref. 25, 27 and 28) according to the formula:

$$\begin{aligned} \Delta_2 F'' = & \left(4B'' - 6D'' + \frac{27}{4}H'' + \frac{27}{4}L''\right) \left(J + \frac{1}{2}\right) \\ & + (-8D'' + 34H'' + 75L'') \left(J + \frac{1}{2}\right)^3 \\ & + (12H'' + 100L'') \left(J + \frac{1}{2}\right)^5 + 16L'' \left(J + \frac{1}{2}\right)^7 + \dots \end{aligned} \quad (3)$$

where  $J$  is the rotational quantum number of the upper energy level. The ground state rotational energies can be reproduced by the newly obtained spectroscopic constants and those given by Long *et al.*<sup>6</sup> (see Table 2) for  $J \leq 48$  within 1 kHz. While the difference increases with  $J$  and reaches 212 kHz for  $J = 72$  due to the absence of the higher centrifugal distortion constant  $L_v$  in the parameters in ref. 6.

Thereby, the ro-vibrational constants of the 30013 state were derived from a fit of 72 transition frequencies with the refined ground state constants determined in this work. The fit resulted in eight parameters with root mean squares (RMSs) of 4.6 kHz given in Table 2. Analogous fits were applied to line positions of the other four cold bands 00011–00001,<sup>27,29</sup> 10011–00001,<sup>28</sup> 10012–00001,<sup>25</sup> and 30012–00001<sup>5</sup> measured with sub-MHz accuracy with the new ground state constants. The spectroscopic parameters retrieved from the fit are summarized in Table 2. The line position differences  $\Delta_{(\text{cal.}-\text{exp.})}$  between those calculated from the spectroscopic parameters and the experimental values are shown in panels (a), (b), (c), (d) and (e) of Fig. 6 for 00011–00001, 10011–00001 and 10012–00001, 30012–00001 and 30013–00001 bands, respectively. As shown in Fig. 6, most of the differences are located within the  $3\text{-}\sigma$  regions (brown shadows). In particular, the differences of all transitions in the 10012 and 30013 are less than 20 kHz, and smaller than the respective  $2\text{-}\sigma$

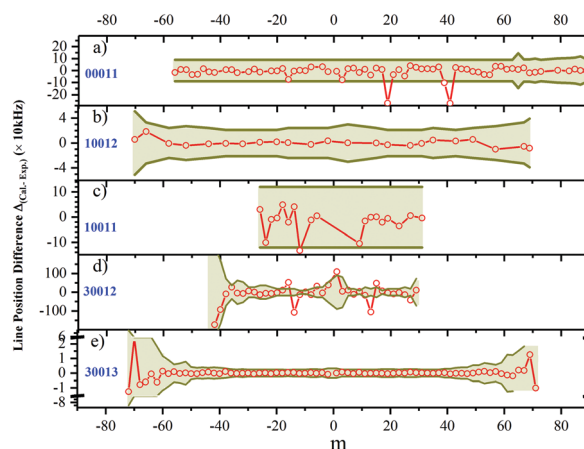


Fig. 6 Line position differences  $\Delta$  between those calculated from the spectroscopic parameters and the experimental values versus the quantum number  $m$  for 00011–00001 (S), 10012–00001 (S), 10011–00001 (S), 30012–00001 (D), and 30013–00001 (S) cold bands. The brown shadows represent the  $3\text{-}\sigma$  uncertainty regions. S: saturated Doppler-free spectroscopy; D: Doppler-limited spectroscopy.

uncertainties. The differences over  $3\text{-}\sigma$  uncertainty regions indicate that either the experimental uncertainties are underestimated, or there is a perturbation around the ro-vibrational state. Therefore, positions of R(18), R(38), R(40) in the 00011–00001 band, P(12) in the 10011–00001 band, P(6), R(0), R(26) in the 30012–00001 band are found to have discrepancies larger than  $3\text{-}\sigma$  experimental uncertainties. A small perturbation was found occurring at  $J' = 13$  or 15 by Long *et al.*<sup>5</sup> with the comparison of their measured transition frequencies to HITRAN2012.<sup>43</sup> As can be seen in Fig. 6d, this perturbation not only leads to a deviation of more than 1 MHz for these two levels, but also creates influence on neighboring levels ( $J' = 11, 17$ ). The comparisons show that the 00011, 10011, 10012, and 30013 states are free from perturbations at the kHz levels.

Using the Lodi-Tennyson methodology, Zak *et al.*<sup>16</sup> gave good predictions of line intensities of some perturbed transitions in the 20012–00001, 21113–01101 bands compared with the Fourier-Transform spectroscopy measurements,<sup>18</sup> but failed in

Table 2 Fitted spectroscopic constants for 00001, 00011, 10012, 10011, 30013 and 30012 states of  $^{12}\text{C}^{16}\text{O}_2$

	00001	00011 <sup>S27,29</sup>	10012 <sup>S25</sup>	10011 <sup>S28</sup>	30013 <sup>S5</sup>	30012 <sup>D5</sup>
$G_v$ (MHz)	—	70425529.0588(88)	108310239.5010(46)	111366358.075(34)	186708240.74732(36)	190303782.265(29)
$B_v$ (kHz)	11698469.9972(97)	11606206.955(23)	11617053.162(17)	11603861.78(30)	11593307.0751(42)	11585628.23(27)
$D_v$ (Hz)	3998.6294(96)	3998.061(14)	4723.714(17)	3425.21(73)	5143.476(13)	2941.78(59)
$H_v$ (mHz)	0.4133(35)	0.4424(30)	6.6919(61)	5.26(48)	29.728(18)	15.24(32)
$L_v$ ( $\mu\text{Hz}$ )	−0.00056(42)	−0.00036(20)	−0.02536(67)	[−0.00056]	0.209(11)	[−0.00056]
$M_v$ ( $\times 10^{-10}$ Hz)	—	—	—	—	0.302(37)	—
$N_v$ ( $\times 10^{-14}$ Hz)	—	—	—	—	−0.161(61)	—
$O_v$ ( $\times 10^{-18}$ Hz)	—	—	—	—	0.439(39)	—
Intensity range ( $\times 10^{-25}$ cm mol <sup>−1</sup> )	—	$59\text{--}3.3 \times 10^7$	$245\text{--}3.6 \times 10^5$	$3.1 \times 10^5\text{--}5.9 \times 10^5$	0.064–173	22–178
$J_{\text{max}}$	72	90	70	30	72	42
$n/N$	67/72	64/67	23/23	18/19	72/72	28/36
RMS (kHz)	16.4	22.5	6.8	48.0	4.6	376

The uncertainty (one standard deviation) in the last digits is in parentheses. S: Saturated spectroscopy. D: Doppler-limited spectroscopy. The intensity range is for the transitions observed in the respective reference.  $n/N$ :  $n$  is the number of transitions included in the fit,  $N$  is the number of measured transitions. RMS: root-mean-square.

reproductions of the line intensities in the 30012–00001 band at the level of 0.5%, although the resonance in the 30012 vibrational state is very small. In general, we can expect larger uncertainties of intensities for the transitions affected by the perturbations. Meanwhile, line intensities of transitions from an unperturbed vibrational state, such as those in the 00011–00001 and 30013–00001 bands could potentially be predicted with better accuracy in the future. Therefore, these transitions would be used as better reference candidates for passive remote sensing.

## 4. Conclusion

Here we presented a precision spectroscopy study using a laser-locked cavity ring-down spectrometer referenced to an optical frequency comb. It allowed us to record the Doppler-free absorption spectra of the P(72)–R(70) 72 lines in the 30013–00001 band of  $^{12}\text{C}^{16}\text{O}_2$ . The line centers were determined with an accuracy of a few kHz for the lines with a wide intensity range by three orders of magnitude. To the best of our knowledge, the weakest line (line intensity in the order of  $10^{-27}$  cm molecule $^{-1}$  at 296 K) was so far detected by saturated molecular absorption spectroscopy. In total, 67 ground state combination differences from 134 experimental Lamb-dip frequencies of four cold bands were used to refine the ground spectroscopic constants, which led to more independent spectroscopic parameters of the 0001, 10011, 10012, 30012 and 30013 vibrational states. The high precision line positions may not only be used as frequency standards but also be beneficial for the study of the advanced line profiles taking into account the effects such as speed dependence, collisional narrowing, and line mixing relevant to remote sensing.<sup>1</sup>

## Conflicts of interest

There are no conflicts to declare.

## Acknowledgements

This work was jointly supported by NSFC (21473172, 91436209 and 21688102) and CAS (XDB21020100).

## Notes and references

- C. E. Miller, D. Crisp, P. L. DeCola, S. C. Olsen, J. T. Randerson, A. M. Michalak, A. Alkhaled, P. Rayner, D. J. Jacob, P. Suntharalingam, D. B. A. Jones, A. S. Denning, M. E. Nicholls, S. C. Doney, S. Pawson, H. Boesch, B. J. Connor, I. Y. Fung, D. O'Brien, R. J. Salawitch, S. P. Sander, B. Sen, P. Tans, G. C. Toon, P. O. Wennberg, S. C. Wofsy, Y. L. Yung and R. M. Law, Precision requirements for space-based XCO<sub>2</sub> data, *J. Geophys. Res.: Atmos.*, 2007, **112**, 1–19.
- A. Kuze, H. Suto, M. Nakajima and T. Hamazaki, Thermal and near infrared sensor for carbon observation Fourier-transform spectrometer on the Greenhouse Gases Observing Satellite for greenhouse gases monitoring, *Appl. Opt.*, 2009, **48**, 6716–6733.
- T. Delahaye, M. Ghysels, J. T. Hodges, K. Sung, R. Armante and H. Tran, Measurement and Modeling of Air-Broadened Methane Absorption in the MERLIN Spectral Region at Low Temperatures, *J. Geophys. Res.: Atmos.*, 2019, **124**, 3556–3564.
- P. F. Bernath, Journal of Quantitative Spectroscopy & Radiative Transfer The Atmospheric Chemistry Experiment (ACE), *J. Quant. Spectrosc. Radiat. Transfer*, 2017, **186**, 3–16.
- D. A. Long, S. Wójtewicz, C. E. Miller and J. T. Hodges, Frequency-agile, rapid scanning cavity ring-down spectroscopy (FARS-CRDS) measurements of the (30012) ← (00001) near-infrared carbon dioxide band, *J. Quant. Spectrosc. Radiat. Transfer*, 2015, **161**, 35–40.
- D. A. Long, G.-W. Truong, J. T. Hodges and C. E. Miller, Absolute  $^{12}\text{C}^{16}\text{O}_2$  transition frequencies at the kHz-level from 1.6 to 7.8  $\mu\text{m}$ , *J. Quant. Spectrosc. Radiat. Transfer*, 2013, **130**, 112–115.
- J. Burkart, T. Sala, D. Romanini, M. Marangoni, A. Campargue and S. Kassi, Saturated CO<sub>2</sub> absorption near 1.6  $\mu\text{m}$  for kilohertz-accuracy transition frequencies, *J. Chem. Phys.*, 2015, **142**, 191103.
- C. E. Miller and L. R. Brown, Near infrared spectroscopy of carbon dioxide I.  $^{16}\text{O}^{12}\text{C}^{16}\text{O}$  line positions, *J. Mol. Spectrosc.*, 2004, **228**, 329–354.
- N. Picqué and T. W. Hänsch, Frequency comb spectroscopy, *Nat. Photonics*, 2019, **13**, 146–157.
- O. L. Polyansky, K. Bielska, M. Ghysels, L. Lodi, N. F. Zobov, J. T. Hodges and J. Tennyson, High-Accuracy CO<sub>2</sub> Line Intensities Determined from Theory and Experiment, *Phys. Rev. Lett.*, 2015, **114**, 1–5.
- V. M. Devi, D. C. Benner, K. Sung, L. R. Brown, T. J. Crawford, C. E. Miller, B. J. Drouin, V. H. Payne, S. Yu, M. A. H. Smith, A. W. Mantz and R. R. Gamache, Line parameters including temperature dependences of self- and air-broadened line shapes of  $^{12}\text{C}^{16}\text{O}_2$ : 1.6- $\mu\text{m}$  region, *J. Quant. Spectrosc. Radiat. Transfer*, 2016, **177**, 117–144.
- T. A. Odintsova, E. Fasci, L. Moretti, E. J. Zak, O. L. Polyansky, J. Tennyson, L. Gianfrani and A. Castrillo, Highly accurate intensity factors of pure CO<sub>2</sub> lines near 2  $\mu\text{m}$ , *J. Chem. Phys.*, 2017, **146**, 244309.
- H. Yi, Q. Liu, L. Gameson, A. J. Fleisher and J. T. Hodges, High-accuracy  $^{12}\text{C}^{16}\text{O}_2$  line intensities in the 2  $\mu\text{m}$  wavelength region measured by frequency-stabilized cavity ring-down spectroscopy, *J. Quant. Spectrosc. Radiat. Transfer*, 2018, **206**, 367–377.
- A. J. Fleisher, E. M. Adkins, Z. D. Reed, H. Yi, D. A. Long, H. M. Fleurbaey and J. T. Hodges, Twenty-Five-Fold Reduction in Measurement Uncertainty for a Molecular Line Intensity, *Phys. Rev. Lett.*, 2019, **123**, 043001.
- X. Huang, D. W. Schwenke, R. S. Freedman and T. J. Lee, Ames-2016 line lists for 13 isotopologues of CO<sub>2</sub>: Updates, consistency, and remaining issues, *J. Quant. Spectrosc. Radiat. Transfer*, 2017, **203**, 224–241.
- E. Zak, J. Tennyson, O. L. Polyansky, L. Lodi, N. F. Zobov, S. A. Tashkun and V. I. Perevalov, A room temperature CO<sub>2</sub> line list with ab initio computed intensities, *J. Quant. Spectrosc. Radiat. Transfer*, 2016, **177**, 31–42.
- S. A. Tashkun, V. I. Perevalov, R. R. Gamache and J. Lamouroux, CDS-296, high-resolution carbon dioxide

- spectroscopic databank: An update, *J. Quant. Spectrosc. Radiat. Transfer*, 2019, **228**, 124–131.
- 18 R. A. Toth, L. R. Brown, C. E. Miller, V. M. Devi and D. C. Benner, Line strengths of  $^{12}\text{C}^{16}\text{O}_2$ : 4550–7000  $\text{cm}^{-1}$ , *J. Mol. Spectrosc.*, 2006, **239**, 221–242.
  - 19 R. Guo, J. Teng, K. Cao, H. Dong, W. Cui and T. Zhang, Comb-assisted, Pound-Drever-Hall locked cavity ring-down spectrometer for high-performance retrieval of transition parameters, *Opt. Express*, 2019, **27**, 31850.
  - 20 L. Lodi and J. Tennyson, Line lists for  $\text{H}_2^{18}\text{O}$  and  $\text{H}_2^{17}\text{O}$  based on empirical line positions and ab initio intensities, *J. Quant. Spectrosc. Radiat. Transfer*, 2012, **113**, 850–858.
  - 21 A. W. Liu, X. F. Li, J. Wang, Y. Lu, C. F. Cheng, Y. R. Sun and S.-M. Hu, The  $4\nu_{\text{CH}}$  overtone of  $^{12}\text{C}_2\text{H}_2$ : Sub-MHz precision spectrum reveals perturbations The  $4\nu_{\text{CH}}$  overtone of  $^{12}\text{C}_2\text{H}_2$ : Sub-MHz precision spectrum, *J. Chem. Phys.*, 2013, **014312**, 6–10.
  - 22 S. Twagirayezu, M. J. Cich, T. J. Sears, C. P. McRaven and G. E. Hall, Frequency-comb referenced spectroscopy of  $\nu_4$ - and  $\nu_5$ -excited hot bands in the 1.5  $\mu\text{m}$  spectrum of  $\text{C}_2\text{H}_2$ , *J. Mol. Spectrosc.*, 2015, **316**, 64–71.
  - 23 C. C. Chou, A. G. Maki, S. J. Tochitsky, J. T. Shy, K. M. Evenson and L. R. Zink, Frequency Measurements and Molecular Constants of  $\text{CO}_2$  0002-[1001,0201]<sub>I,II</sub> Sequence Band Transitions, *J. Mol. Spectrosc.*, 1995, **172**, 233–242.
  - 24 I. Galli, M. Siciliani De Cumis, F. Cappelli, S. Bartalini, D. Mazzotti, S. Borri, A. Montori, N. Akikusa, M. Yamanishi, G. Giusfredi, P. Cancio and P. De Natale, Comb-assisted sub-kilohertz linewidth quantum cascade laser for high-precision mid-infrared spectroscopy, *Appl. Phys. Lett.*, 2013, **102**, 121117.
  - 25 Y.-C. Guan, D. N. Patel, B.-H. Peng, T.-H. Suen, L.-B. Wang and J.-T. Shy, Frequency measurements and molecular constants of the  $^{12}\text{C}^{16}\text{O}_2$  [1001, 0201]<sub>II</sub>  $\leftarrow$  0000 band near 2.7  $\mu\text{m}$ , *J. Mol. Spectrosc.*, 2017, **334**, 26–30.
  - 26 A. Amy-Klein, H. Vigué and C. Chardonnet, Absolute frequency measurement of  $^{12}\text{C}^{16}\text{O}_2$  laser lines with a femtosecond laser comb and new determination of the  $^{12}\text{C}^{16}\text{O}_2$  molecular constants and frequency grid, *J. Mol. Spectrosc.*, 2004, **228**, 206–212.
  - 27 C.-C. Liao, K.-Y. Wu, Y.-H. Lien and J.-T. Shy, in *Proceedings of the 63rd Ohio state university international symposium on molecular spectroscopy*, Columbus, Ohio, 2008, <https://kb.osu.edu/handle/1811/33348>.
  - 28 K.-Y. Wu, C.-C. Liao, Y.-H. Lien and J.-T. Shy, in *Proceedings of the 63rd Ohio state university international symposium on molecular spectroscopy*, Columbus, Ohio, 2008, <https://kb.osu.edu/handle/1811/33349>.
  - 29 W.-J. Ting, P.-L. Luo, C.-H. Chung, H.-C. Chen, Y.-H. Lien and J.-T. Shy, in *Proceedings of the 64th Ohio state university international symposium on molecular spectroscopy*, Columbus, Ohio, 2009, <https://kb.osu.edu/handle/1811/37970>.
  - 30 G. Giusfredi, S. Bartalini, S. Borri, P. Cancio, I. Galli, D. Mazzotti and P. De Natale, Saturated-absorption cavity ring-down spectroscopy, *Phys. Rev. Lett.*, 2010, **104**, 1–4.
  - 31 H.-C. Chen, C.-Y. Hsiao, W.-J. Ting, S.-T. Lin and J.-T. Shy, Saturation spectroscopy of  $\text{CO}_2$  and frequency stabilization of an optical parametric oscillator at 2.77  $\mu\text{m}$ , *Opt. Lett.*, 2012, **37**, 2409.
  - 32 F. Cappelli, I. Galli, S. Borri, G. Giusfredi, P. Cancio, D. Mazzotti, A. Montori, N. Akikusa, M. Yamanishi, S. Bartalini and P. De Natale, Subkilohertz linewidth room-temperature mid-infrared quantum cascade laser using a molecular sub-Doppler reference, *Opt. Lett.*, 2012, **37**, 4811.
  - 33 I. Galli, S. Bartalini, P. C. Pastor, F. Cappelli, G. Giusfredi, D. Mazzotti, N. Akikusa, M. Yamanishi and P. De Natale, Absolute frequency measurements of  $\text{CO}_2$  transitions at 4.3  $\mu\text{m}$  with a comb-referenced quantum cascade laser, *Mol. Phys.*, 2013, **111**, 2041–2045.
  - 34 G. W. Truong, D. A. Long, A. Cygan, D. Lisak, R. D. Van Zee and J. T. Hodges, Comb-linked, cavity ring-down spectroscopy for measurements of molecular transition frequencies at the kHz-level, *J. Chem. Phys.*, 2013, **138**, 094201.
  - 35 J. Wang, Y. R. Sun, L. G. Tao, A. W. Liu, T. P. Hua, F. Meng and S. M. Hu, Comb-locked cavity ring-down saturation spectroscopy, *Rev. Sci. Instrum.*, 2017, **88**, 043108.
  - 36 L. G. Tao, A. W. Liu, K. Pachucki, J. Komasa, Y. R. Sun, J. Wang and S. M. Hu, Toward a Determination of the Proton-Electron Mass Ratio from the Lamb-Dip Measurement of HD, *Phys. Rev. Lett.*, 2018, **120**, 1–5.
  - 37 J. Wang, Y. R. Sun, L. G. Tao, A. W. Liu and S. M. Hu, Communication: Molecular near-infrared transitions determined with sub-kHz accuracy, *J. Chem. Phys.*, 2017, **147**, 091103.
  - 38 L. S. Ma, J. Ye, P. Dubé and J. L. Hall, Ultrasensitive frequency-modulation spectroscopy enhanced by a high-finesse optical cavity: theory and application to overtone transitions of  $\text{C}_2\text{H}_2$  and  $\text{C}_2\text{HD}$ , *J. Opt. Soc. Am. B*, 1999, **16**, 2255.
  - 39 I. E. Gordon, L. S. Rothman, C. Hill, R. V. Kochanov, Y. Tan, P. F. Bernath, M. Birk, V. Boudon, A. Campargue, K. V. Chance, B. J. Drouin, J. M. Flaud, R. R. Gamache, J. T. Hodges, D. Jacquemart, V. I. Perevalov, A. Perrin, K. P. Shine, M. A. H. Smith, J. Tennyson, G. C. Toon, H. Tran, V. G. Tyuterev, A. Barbe, A. G. Császár, V. M. Devi, T. Furtenbacher, J. J. Harrison, J. M. Hartmann, A. Jolly, T. J. Johnson, T. Karman, I. Kleiner, A. A. Kyuberis, J. Loos, O. M. Lyulin, S. T. Massie, S. N. Mikhailenko, N. Moazzen-Ahmadi, H. S. P. Müller, O. V. Naumenko, A. V. Nikitin, O. L. Polyansky, M. Rey, M. Rotger, S. W. Sharpe, K. Sung, E. Starikova, S. A. Tashkun, J. Vander Auwera, G. Wagner, J. Wilzewski, P. Wcisło, S. Yu and E. J. Zak, The HITRAN2016 molecular spectroscopic database, *J. Quant. Spectrosc. Radiat. Transfer*, 2017, **203**, 3–69.
  - 40 S. Kassı and A. Campargue, Cavity ring down spectroscopy with  $5 \times 10^{-13} \text{ cm}^{-1}$  sensitivity, *J. Chem. Phys.*, 2012, **137**, 0–6.
  - 41 L. G. Tao, T. P. Hua, Y. R. Sun, J. Wang, A. W. Liu and S. M. Hu, Frequency metrology of the acetylene lines near 789 nm from lamb-dip measurements, *J. Quant. Spectrosc. Radiat. Transfer*, 2018, **210**, 111–115.
  - 42 J. Chen, T. P. Hua, L. G. Tao, Y. R. Sun, A. W. Liu and S. M. Hu, Absolute frequencies of water lines near 790 nm with  $10^{-11}$  accuracy, *J. Quant. Spectrosc. Radiat. Transfer*, 2018, **205**, 91–95.
  - 43 L. S. Rothman, I. E. Gordon, Y. Babikov, A. Barbe, D. Chris Benner, P. F. Bernath, M. Birk, L. Bizzocchi, V. Boudon,

- L. R. Brown, A. Campargue, K. Chance, E. A. Cohen, L. H. Coudert, V. M. Devi, B. J. Drouin, A. Fayt, J. M. Flaud, R. R. Gamache, J. J. Harrison, J. M. Hartmann, C. Hill, J. T. Hodges, D. Jacquemart, A. Jolly, J. Lamouroux, R. J. Le Roy, G. Li, D. A. Long, O. M. Lyulin, C. J. Mackie, S. T. Massie, S. Mikhailenko, H. S. P. Müller, O. V. Naumenko, A. V. Nikitin, J. Orphal, V. Perevalov, A. Perrin, E. R. Polovtseva, C. Richard, M. A. H. Smith, E. Starikova, K. Sung, S. Tashkun, J. Tennyson, G. C. Toon, V. G. Tyuterev and G. Wagner, The HITRAN2012 molecular spectroscopic database, *J. Quant. Spectrosc. Radiat. Transfer*, 2013, **130**, 4–50.
- 44 R. L. Barger and J. L. Hall, Pressure Shift and Broadening of Methane Line at 3.39  $\mu\text{m}$  Studied by Laser-Saturated Molecular Absorption, *Phys. Rev. Lett.*, 1969, **22**, 4–8.
- 45 V. P. Chebotayev, Supernarrow saturated absorption resonances, *Phys. Rep.*, 1985, **119**, 75–116.
- 46 A. T. Mattick, N. A. Kurnit and A. Javan, Velocity dependence of collision broadening cross sections in  $\text{NH}_3$ , *Chem. Phys. Lett.*, 1976, **38**, 176–180.
- 47 T. W. Meyer, C. K. Rhodes and H. A. Haus, High-resolution line broadening and collisional studies in  $\text{CO}_2$  using non-linear spectroscopic techniques, *Phys. Rev. A: At., Mol., Opt. Phys.*, 1975, **12**, 1993–2008.
- 48 L. S. Vasilenko, V. P. Kochanov and V. P. Chebotayev, Non-linear dependence of optical resonance widths at  $\text{CO}_2$  transitions on pressure, *Opt. Commun.*, 1977, **20**, 409–411.
- 49 M. V. Belyaev, L. S. Vasilenko, M. N. Skvortsov and V. P. Chebotayev, Resonant coherent transient process in a gas subjected to a standing wave field, *Sov. Phys.-JETP*, 1981, **81**, 526–539.
- 50 S. Twagirayezu, G. E. Hall and T. J. Sears, Frequency measurements and self-broadening of sub-Doppler transitions in the  $\nu_1 + \nu_3$  band of  $\text{C}_2\text{H}_2$ , *J. Chem. Phys.*, 2018, **149**, 154308.
- 51 V. A. Alekseev and L. P. Yatsenko, Effect of field and transit broadening on the collisional displacement of an optical frequency standard, *JEPT Lett.*, 1979, **29**, 428–432.
- 52 V. A. Alekseev, T. L. Andreeva and I. I. Sobel'man, Contribution to the theory of nonlinear power resonances in gas lasers, *Sov. Phys.-JETP*, 1973, **64**, 813–824.
- 53 A. A. Madej, A. J. Alcock, A. Czajkowski, J. E. Bernard and S. Chepurov, Accurate absolute reference frequencies from 1511 to 1545 nm of the  $\nu_1 + \nu_3$  band of  $^{12}\text{C}_2\text{H}_2$  determined with laser frequency comb interval measurements, *J. Opt. Soc. Am. B*, 2006, **23**, 2200.
- 54 C. S. Edwards, H. S. Margolis, G. P. Barwood, S. N. Lea, P. Gill and W. R. C. Rowley, High-accuracy frequency atlas of  $^{13}\text{C}_2\text{H}_2$  in the 1.5  $\mu\text{m}$  region, *Appl. Phys. B: Lasers Opt.*, 2005, **80**, 977–983.
- 55 A. A. Madej, J. E. Bernard, A. John Alcock, A. Czajkowski and S. Chepurov, Accurate absolute frequencies of the  $\nu_1 + \nu_3$  band of  $^{13}\text{C}_2\text{H}_2$  determined using an infrared mode-locked Cr:YAG laser frequency comb, *J. Opt. Soc. Am. B*, 2006, **23**, 741.